CrossMark
click for updates

Gold Nanoparticle Conjugation Enhances the Antiacanthamoebic Effects of Chlorhexidine

Yousuf Aqeel,[a] Ruqaiyyah Siddiqui,[b] Ayaz Anwar,[c] Muhammad Raza Shah,[c] Naveed Ahmed Khan[b]

Department of Molecular and Cell Biology, School of Medicine, Boston University, Boston, Massachusetts, USA[a]; Department of Biological Sciences, Faculty of Science and Technology, Sunway University, Bandar Sunway, Malaysia[b]; International Center for Chemical and Biological Sciences, H.E.J. Research Institute of Chemistry, University of Karachi, Karachi, Pakistan[c]

Acanthamoeba keratitis is a serious infection with blinding consequences and often associated with contact lens wear. Early diagnosis, followed by aggressive topical application of drugs, is a prerequisite in successful treatment, but even then prognosis remains poor. Several drugs have shown promise, including chlorhexidine gluconate; however, host cell toxicity at physiologically relevant concentrations remains a challenge. Nanoparticles, subcolloidal structures ranging in size from 10 to 100 nm, are effective drug carriers for enhancing drug potency. The overall aim of the present study was to determine whether conjugation with gold nanoparticles enhances the antiacanthamoebic potential of chlorhexidine. Gold-conjugated chlorhexidine nanoparticles were synthesized. Briefly, gold solution was mixed with chlorhexidine and reduced by adding sodium borohydride, resulting in an intense deep red color, indicative of colloidal gold-conjugated chlorhexidine nanoparticles. The synthesis was confirmed using UV-visible spectrophotometry that shows a plasmon resonance peak of 500 to 550 nm, indicative of gold nanoparticles. Further characterization using matrix-assisted laser desorption ionization-mass spectrometry showed a gold-conjugated chlorhexidine complex at *m/z* 699 ranging in size from 20 to 100 nm, as determined using atomic force microscopy. To determine the amoebicidal and amoebistatic effects, amoebae were incubated with gold-conjugated chlorhexidine nanoparticles. For controls, amoebae also were incubated with gold and silver nanoparticles alone, chlorhexidine alone, neomycin-conjugated nanoparticles, and neomycin alone. The findings showed that gold-conjugated chlorhexidine nanoparticles exhibited significant amoebicidal and amoebistatic effects at 5 μM. Amoebicidal effects were observed by parasite viability testing using a Trypan blue exclusion assay and flow-cytometric analysis using propidium iodide, while amoebistatic effects were observed using growth assays. In contrast, chlorhexidine alone, at a similar concentration, showed limited effects. Notably, neomycin alone or conjugated with nanoparticles did not show amoebicidal or amoebistatic effects. Pretreatment of *A. castellanii* with gold-conjugated chlorhexidine nanoparticles reduced amoeba-mediated host cell cytotoxicity from 90% to 40% at 5 μM. In contrast, chlorhexidine alone, at similar concentrations, had no protective effects for the host cells. Similarly, amoebae treated with neomycin alone or neomycin-conjugated nanoparticles showed no protective effects. Overall, these findings suggest that gold-conjugated chlorhexidine nanoparticles hold promise in the improved treatment of *A. castellanii* keratitis.

*A*canthamoeba is a free-living opportunistic pathogen that has gained significant clinical attention over the past few years. It is a causative agent of fatal granulomatous amoebic encephalitis in immunocompromised individuals and causes a sight-threatening keratitis in contact lens wearers (1–3). The treatment includes the use of a combination of drugs, including chlorhexidine digluconate, neomycin, propamidine isethionate, 5-fluorocytosine, polyhexamethylene biguanide, and pentamidine isethionate (3–5). However, these drugs may exhibit side effects at recommended concentrations. For example, mature cataracts and iris atrophy developed in *Acanthamoeba* keratitis patients due to the use of 0.02% chlorhexidine and 0.01% propamidine isethionate (6). Similarly, 5-fluorocytosine and pentamidine isethionate caused hematologic damage and nephrotoxicity in immunocompromised patients with amoebic infections (7, 8). Among various drugs, chlorhexidine digluconate is the most commonly used drug in the treatment of *Acanthamoeba* keratitis. Chlorhexidine is a polybiguanide compound, commonly present in the form of salts such as chlorhexidine digluconate. It is an antiseptic agent used in mouthwashes, as a skin cleanser in surgical scrubs, and in germicidal hand washes. It acts by releasing a positive chlorhexidine cation under physiological pH that reacts with the negatively charged plasma membrane, resulting in membrane structure and

permeability changes that cause ionic leakage, cytoplasmic disruption, and, ultimately, cell death. It is readily used in the treatment of *Acanthamoeba* keratitis at a concentration of 0.02%, which exhibits both trophicidal and cysticidal effects (9).

Nanoparticles are subcolloidal structures ranging in size from 10 to 100 nm and are effective drug carriers for enhancing drug potency. By controlling the structure precisely at nanoscale dimensions, their surface structure is modified, which can help in the improved bioavailability of poorly absorbed drugs and enable them to be delivered efficiently. Antimicrobial formulation in the form of nanoparticles is shown to act as an effective bactericidal

material against Gram-positive and Gram-negative bacteria ([10–12]). Gold (Au) nanoparticles with well-developed surface chemistry, controllable geometry, and chemical stability are excellent tools to be used in biological studies. The overall aim of the present study was to determine whether conjugation with gold nanoparticles can enhance the antiacanthamoebic effects of chlorhexidine digluconate.

MATERIALS AND METHODS

***Acanthamoeba castellanii* cultures.** All chemicals were purchased from Sigma (Poole, Dorset, England), unless otherwise stated. Chlorhexidine digluconate (282227) (>99% purity) and neomycin trisulfate salt hydrate (N6386) (>95% purity) were used in the present study. A keratitis isolate of *A. castellanii* belonging to the T4 genotype was purchased from the American Type Culture Collection (ATCC 50492). Amoebae were routinely grown in 10 ml PYG medium (0.75% [wt/vol] proteose peptone, 0.75% [wt/vol] yeast extract, 1.5% [wt/vol] glucose) in T75 75-cm² tissue culture flasks at 30°C ([13]). The medium was changed 18 h before the experiment, and amoebae adherent to the flask, representing the trophozoite form, were collected by placing it on ice for 20 min with gentle agitation and used in all experiments.

HBMEC cultures. The brain microvascular cells were of human origin and cultured as described previously ([14], [15]). The endothelial cells were purified using fluorescent-activated cell sorting (FACS), and their purity was checked by the expression of endothelial markers such as F-VIII and carbonic anhydrase IV and the uptake of acetylated low-density lipoprotein (Dil-AcLDL), resulting in more than 99% pure endothelial cultures. The human brain microvascular endothelial cells (HBMEC) were routinely grown in rat tail collagen-coated tissue culture dishes in RPMI 1640 containing 10% heat-inactivated fetal bovine serum, 10% Nu-Serum, 2 mM glutamine, 1 mM Na-pyruvate, 100 U penicillin/ml, 100 µg streptomycin/ml, nonessential amino acids (glycine, L-alanine, L-asparagine, L-aspartic acid, L-glutamic acid, L-proline, and L-serine), and vitamins (choline chloride, D-calcium pantothenate, folic acid, nicotinamide, pyridoxal hydrochloride, riboflavin, thiamine hydrochloride, and I-inositol) and incubated at 37°C in a 5% CO_2 incubator. For cytotoxicity assays, HBMEC (10^6 cells/ml/well) were incubated for 24 h until the confluent monolayers were formed and used in all subsequent experiment.

Synthesis of nanoparticles. Initially, gold (Au) and silver (Ag) were selected as metallic carrier due to their inert nature in biological systems and synthesized at a stock concentration of 10 mM. In order to synthesize Au-conjugated chlorhexidine nanoparticles, 5 ml (1 mM) of gold(III) chloride trihydrate solution was added to 5 ml (1 mM) of chlorhexidine solution, and the mixture was placed on a shaker. After 10 min, 30 µl (10 mM) aqueous sodium borohydride was added as a reducing agent. The intense deep red color, characteristic of colloidal gold nanoparticles, was obtained instantly on its addition. The solution was placed on a stirrer for an additional 2 h. After this, UV-visible spectrophotometry, atomic force microscopy, and matrix-assisted laser desorption-mass spectrometry (MALDI-MS) were performed for the characterization of Au-conjugated chlorhexidine nanoparticles. For Ag-conjugated neomycin, 10 ml (1 mM) silver nitrate aqueous solution was added to 2 ml (1 mM) of neomycin solution, and the mixture was placed on a shaker. After 10 min, 0.5 ml (30 mM) of sodium borohydride was added as a reducing agent and shaking was continued for another 6 h, after which the solution was subjected to characterization using UV-visible spectrophotometry, atomic force microscopy, and MALDI-MS. To determine whether Ag-conjugated chlorhexidine and Au-conjugated neomycin exhibit increased efficacy, attempts were made to conjugate Au with neomycin and Ag with chlorhexidine as described above. Conversely, bare Au and Ag nanoparticles were prepared by reducing it with 30 µl (10 mM) aqueous sodium borohydride just before use.

ESI-MS of nanoparticles. In order to quantify the amount of drug used for conjugation with nanoparticles, electrospray ionization mass spectrometry (ESI-MS) was performed. ESI is also known as soft ionization. High voltage is applied to the liquid medium, which creates aerosols. The ions produced then are passed through the mass spectrometry channel through which mass spectrum is obtained. Briefly, the colloidal solution was collected in a 1.5-ml microcentrifuge tube and centrifuged at full speed to ensure the complete settlement of nanoparticles. The centrifuged material was separated and 0.1% trifluoroacetic acid was added. After this, the sample was injected for mass spectrometry analysis using an Agilent 6460 ESI-MS that was run in positive mode.

Atomic force microscopy of nanoparticles. In order to determine the morphology of nanoparticles, atomic force microscopic analysis was performed as described previously but with slight modifications ([13]). Briefly, a cover glass of 18-mm diameter was rinsed in distilled water, followed by three washes in 70% ethanol. After this, 10 µl of Au-conjugated chlorhexidine and Ag-conjugated neomycin synthesized previously was overlaid on the surface of the coverslip in the biosafety hood at room temperature and incubated until it was dried. The following day, images were obtained using an Agilent 5500 atomic force microscope operated in tapping mode by using a silicon nitride soft cantilever of triangular shape (model MLCT-AUHW; Veeco) having a normal spring of 0.01N per m and 0.1N per m.

Amoebicidal assays. To determine the effects of Au-conjugated chlorhexidine nanoparticles on amoebae, cidal assays were performed as described previously ([16]). Briefly, *A. castellanii* (10^6 amoebae/0.5 ml/well) was incubated with 1 µM, 2.5 µM, 5 µM, 7.5 µM, 10 µM, and 20 µM concentrations of Au-conjugated chlorhexidine nanoparticles and chlorhexidine alone. Additionally, amoebae were incubated with RPMI alone, 20 µM Ag-conjugated neomycin, neomycin alone, Ag nanoparticles, and Au nanoparticles for 24 h at 37°C in 24-well plates. After this incubation, plates were incubated on ice for 20 min, scraped using a rubber policeman, and centrifuged in BD Falcon round-bottom polystyrene tubes at $1,500 \times g$ for 10 min. The pellet was resuspended in 25 mg/liter propidium iodide and incubated for 10 min. Five hundred microliters of phosphate-buffered saline (PBS) was added, and flow-cytometric analysis was performed using a FACSAria III fluorescence-activated cell sorter system (Becton Dickinson, Heidelberg, Germany). The illumination of propidium iodide was recorded using filter 585/42 as previously described ([17]). The dot plots on the graph were gated for phycoerythrin (PE-A) on the horizontal axis and side scattering (SSCeH) on the vertical axis, treated amoebae were superimposed onto analysis gates and compared to controls, and the percent viability was determined on the basis of at least 10,000 events after treatment.

Growth inhibition assays. To determine the effects of Au-conjugated chlorhexidine nanoparticles on the growth of *A. castellanii*, assays were performed as described previously ([18]). Briefly, *A. castellanii* (5×10^5 amoebae/0.5 ml/well) organisms were incubated with various concentrations of Au-conjugated chlorhexidine nanoparticles at 37°C for 48 h. After this incubation, the number of amoebae were determined using hemocytometer counting. For controls, amoebae were incubated in solvent alone, chlorhexidine alone, Ag-conjugated neomycin nanoparticles, and neomycin alone.

Host cell cytotoxicity. To determine antiamoebic effects of Au-conjugated chlorhexidine nanoparticles *in vitro*, assays were performed using HBMEC. *A. castellanii* (5×10^5 amoebae/0.5 ml/well) organisms were pretreated with various concentrations of Au-conjugated chlorhexidine nanoparticles and chlorhexidine alone. Amoebae also were incubated with 20 µM Ag and Au nanoparticles, neomycin, and Ag-conjugated neomycin nanoparticles for 24 h. Amoebae next were collected by centrifugation at $1,000 \times g$ for 5 min. The supernatants were aspirated and pellets resuspended in 0.5 ml of RPMI 1640. This process was repeated 3× to remove any residual drugs. Finally, amoebae were inoculated on HBMEC monolayers grown in 24-well plates. Plates were incubated at 37°C in a 5% CO_2 incubator for 18 h. The next day, cell-free conditioned medium was collected and host cell cytotoxicity was determined by measuring lactate dehydrogenase (LDH) release using a cytotoxicity detection kit (Roche, Indianapolis, IN). The HBMEC incubated alone were used as a negative control, whereas monolayers lysed with 1% Triton X-100 for 30 min at
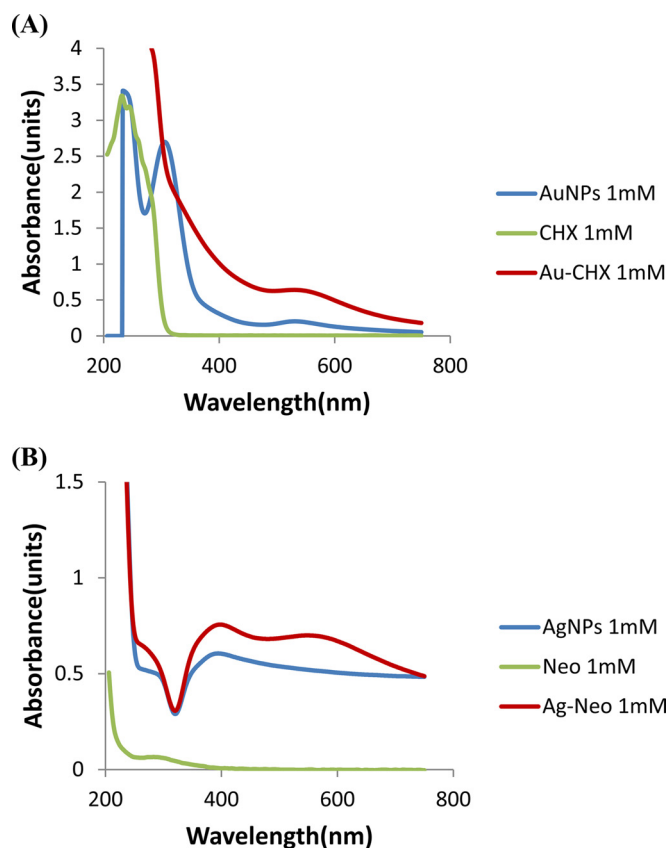
(A)

(B)

FIG 1 Representative UV-visible spectrophotometry of gold (Au)-conjugated chlorhexidine and silver (Ag)-conjugated neomycin showed a surface plasmon resonance band at 500 to 550 nm and 400 to 500 nm. (A) UV-visible spectrophotometry of Au-conjugated chlorhexidine showed a plasmon resonance band at 500 to 550 nm indicative of Au nanoparticles. Conversely, Au alone also showed a band in same region but with lower intensity. Chlorhexidine alone showed a band at around 200 to 250 nm. (B) UV-visible spectrophotometry of Ag-conjugated neomycin showed a plasmon resonance band at around 400 to 450 nm, indicating the synthesis of Ag-conjugated neomycin nanoparticles. Simultaneously, Ag alone also showed a plasmon band at 400 to 450 nm. Furthermore, neomycin alone did not absorb well in the UV spectrum and produced a band of very low intensity at around 250 nm.

37°C were used to represent 100% cell death. The absorbance of samples was converted to percent cytotoxicity using the following equation: (sample value − cells alone)/(total cell death − cells alone) × 100 = percent cytotoxicity.

RESULTS

Synthesis of gold-conjugated chlorhexidine and silver-conjugated neomycin was confirmed using UV-visible spectrophotometry, atomic force microscopy, and MALDI-MS. To determine Au-conjugated chlorhexidine and Ag-conjugated neomycin synthesis, UV visible spectrophotometry, MALDI-MS, and atomic force microscopy were performed. Au-conjugated chlorhexidine and Ag-conjugated neomycin nanoparticles showed UV-visible characteristic surface plasmon resonance bands around 500 to 550 nm and 400 to 500 nm. A comparative UV spectral analysis of Au-conjugated chlorhexidine, Ag-conjugated neomycin, and drug alone is shown (Fig. 1A and B). A drastic enhancement in the absorbance intensity and a small shift in maximum absorbance wavelength (λ_{max}) suggest that chlorhexidine and neomycin were

successfully capped on the Au and Ag surfaces. Further, to quantify the drug, mass spectrometric analysis was done, and it was observed that at this optimized ratio between metal and drug, the entire drug was attached to the metal surface. Sample preparation for ESI-MS analysis showed no peaks for molecular weights of drugs at 505 *m/z* for chlorhexidine and 614 *m/z* for neomycin. Hence, we concluded from this observation that the complete drug is attached to the metal surface and no free drug is present in the colloids (see the figure in the supplemental material). Finally, atomic force microscopy was performed to determine the morphology of particles and their size distribution. Au-conjugated chlorhexidine nanoparticles were found to be spherical and polydisperse in size, ranging from 20 to 100 nm (Fig. 2A). Ag-conjugated neomycin nanoparticles were found to lie in a much narrower size distribution, ranging from 2 to 20 nm (Fig. 2B). Notably, attempts to conjugate Au with neomycin or Ag with chlorhexidine were unsuccessful (data not shown).

Gold-conjugated chlorhexidine nanoparticles exhibited amoebicidal effects. To determine the effects of Au-conjugated chlorhexidine nanoparticles and chlorhexidine alone on the viability of *A. castellanii*, amoebicidal assays were performed. The results revealed that Au-conjugated chlorhexidine nanoparticles exhibited significant amoebicidal effects against *A. castellanii* to 40% at 5 µM ($P < 0.05$ using 2-sample *t* test and two-tailed distribution) (Fig. 3). Similarly, amoebae treated with chlorhexidine alone exhibited cidal effects, and the number of amoebae was reduced to 60% at 5 µM ($P < 0.05$ using 2-sample *t* test and two-tailed distribution) (Fig. 3). In controls, silver-conjugated neomycin nanoparticles and neomycin alone exhibited no effects against *A. castellanii* (Fig. 3). Conversely, treatment with bare gold and silver nanoparticles alone had no observable adverse effects on amoebae (Fig. 3).

Gold-conjugated chlorhexidine nanoparticles inhibited growth of *A. castellanii*. To determine the effects of Au-conjugated chlorhexidine nanoparticles on the growth of *A. castellanii*, assays were performed in the presence of growth medium, i.e., PYG. Au-conjugated chlorhexidine nanoparticles showed inhibitory effects on amoeba growth at 5 µM, and the numbers were significantly reduced ($P < 0.05$ using 2-sample *t* test and two-tailed distribution) (Fig. 4). In contrast, amoebae treated with chlorhexidine alone did not exhibit growth-inhibitory effects at 5 µM ($P > 0.05$ using 2-sample *t* test and two-tailed distribution) (Fig. 4). Controls (amoebae incubated with solvent and bare nanoparticles) showed no inhibitory effects on amoeba growth, and the numbers were doubled after 24 h. Similarly, amoebae incubated with Ag-conjugated neomycin nanoparticles and neomycin alone showed no inhibitory effects on amoeba growth (Fig. 4).

Gold-conjugated chlorhexidine inhibited *A. castellanii*-mediated host cell cytotoxicity. *A. castellanii* cells were pretreated with Au-conjugated chlorhexidine nanoparticles for 24 h in RPMI, followed by host cell cytotoxicity assays. In the absence of any drug, *A. castellanii* produced 90% HBMEC death within 18 h. Pretreatment of *A. castellanii* with Au-conjugated chlorhexidine nanoparticles significantly reduced host cell cytotoxicity to 40% at 5 µM ($P < 0.05$ using 2-sample *t* test and two-tailed distribution) (Fig. 5). In contrast, pretreatment of *A. castellanii* with chlorhexidine did not exhibit significant protective effects at 5 µM ($P < 0.05$ using 2-sample *t* test and two-tailed distribution). Similarly, amoebae treated with Ag-conjugated neomycin nanoparticles and
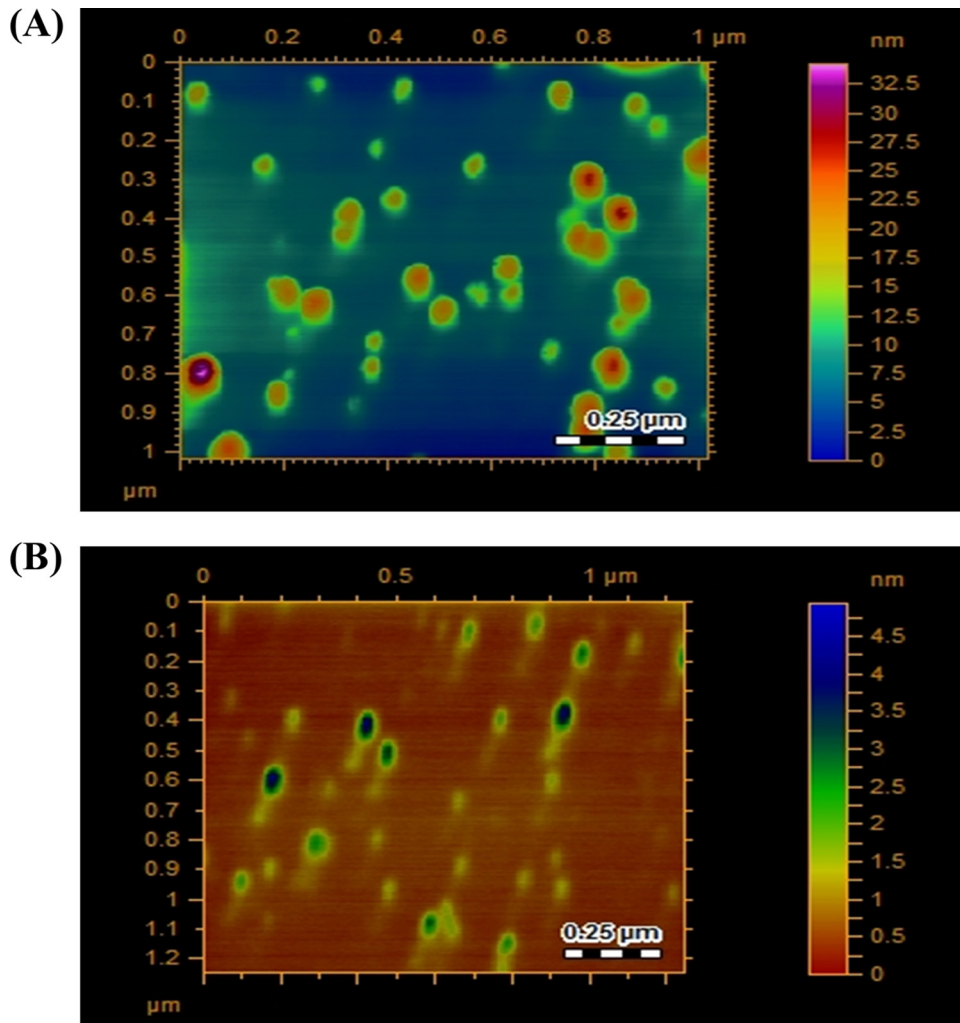
FIG 2 Au-conjugated chlorhexidine ranges in size from 20 to 100 nm, and Ag-conjugated neomycin nanoparticles have sizes from 2 to 20 nm. The particle size varies from 20 to 100 nm. Atomic force microscopy was performed as described in Materials and Methods. Briefly, cover glasses were overlaid with Au-conjugated chlorhexidine and Ag-conjugated neomycin and air dried. On the following day, images were obtained using an Agilent 5500 atomic force microscope. Au-conjugated chlorhexidine nanoparticles were spherical and polydisperse in size within the range of 20 to 100 nm (A), while Ag-conjugated neomycin nanoparticles had a narrower size distribution, ranging from 2 to 20 nm (B). The results are representative of several experiments.

neomycin alone did not show any protective effects for HBMEC against *A. castellanii* (Fig. 5).

DISCUSSION

Among different carriers developed for improved drug delivery, such as liposomes, carbon nanotubes, dendrimers, polymeric micelles, polymeric conjugates, and nanoparticles, only a few have reached clinical applications. It is hoped that drug carriers not only transport the chemotherapeutic agents but also protect drugs from degradation. In particular, the applications of nanoparticles in biomedical research, from diagnostics to therapeutics, in recent years have increased exponentially. Given their small size, high reactivity, as well as translocation into living cells, stability in harsh conditions such as high temperatures offers promise in clinical settings. The most widely used nanoparticles include gold, silver, titanium oxide, and iron nanoparticles (19). As gold is inert, it exhibits weak cytotoxic effects; thus, it is considered the nanoparticle of choice when performing conjugations with various biomolecules and ligands to develop strategies for targeting pathogens (20–22). Cytotoxic drugs can be encapsulated or physically entrapped within a nanosphere or entrapped into a cavity surrounded by nanocapsules (23). Previous studies have developed antimicrobial formulations in the form of nanoparticles that exhibit effective bactericidal effects against Gram-positive and Gram-negative bacteria (10–12). Here, we determined whether conjugation with gold-conjugated nanoparticles enhances the antiacanthamoebic effects of chlorhexidine digluconate. Au-conjugated chlorhexidine and Ag-conjugated neomycin were successfully synthesized that exhibited well-developed surface chemistry, controllable geometry, and chemical stability as determined by UV-visible spectrophotometry, MALDI-MS, and atomic force microscopy.

Amoebicidal assays revealed that although both Au-conjugated chlorhexidine and chlorhexidine alone exhibited amoebicidal properties, Au-conjugated chlorhexidine showed higher levels of toxicity against *A. castellanii* than chlorhexidine alone, 60%
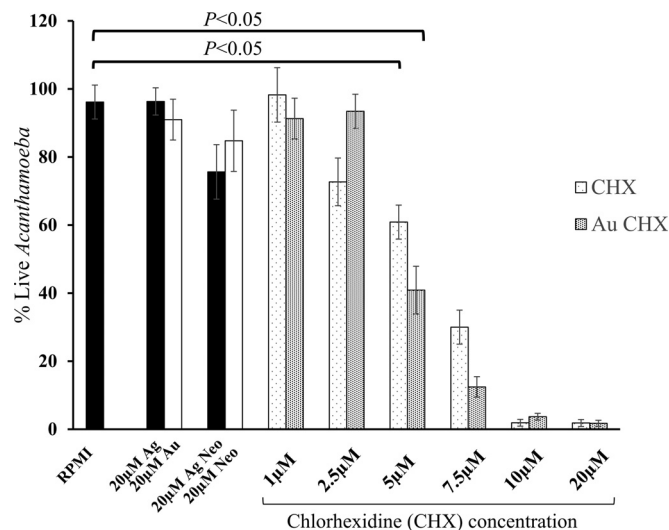
FIG 3 *A. castellanii* cell death was observed by treatment with Au-conjugated chlorhexidine nanoparticles, determined by flow cytometry by propidium iodide staining as described in Materials and Methods. FACS scattergram results are expressed as percent viable *A. castellanii*. Note that Au-conjugated chlorhexidine nanoparticles and chlorhexidine alone exhibited significant anti-acanthamoebic effects at concentrations of 5 μM or higher ($P < 0.05$ using 2-sample t test with two-tailed distribution). The results are expressed as the means ± standard errors from three independent experiments performed in duplicate.

FIG 5 Treatment with Au-conjugated chlorhexidine nanoparticles abolished *A. castellanii*-mediated HBMEC cytotoxicity. Briefly, amoebae (5×10^5 amoebae/0.5 ml/well) were incubated with different concentrations of Au-conjugated chlorhexidine nanoparticles and chlorhexidine alone for 24 h in RPMI and then incubated with HBMEC for 18 h at 37°C in a 5% CO_2 incubator as described in Materials and Methods. The next day, cell-free supernatant was collected and cytotoxicity was determined. The results revealed that pretreatment with Au-conjugated chlorhexidine nanoparticles at 5 μM concentration, but not chlorhexidine alone at 5 μM concentration, abolished *A. castellanii*-mediated HBMEC cytotoxicity. The results are expressed as the means ± standard errors from three independent experiments performed in duplicate.

versus 40%, respectively. The increased cytotoxicity likely is due to the high reactivity of nanoparticles with living cells as well as easy translocation of drug into the living cells, enhancing drug efficacy (24). Chlorhexidine is a positively charged molecule that binds to the negatively charged sites on the cell membrane and destabilizes
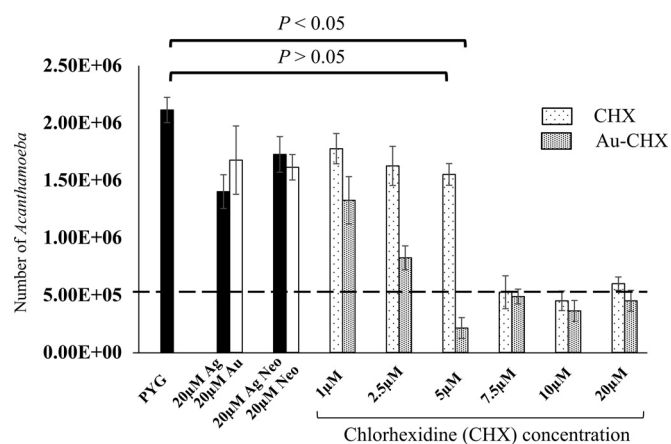

FIG 4 Au-conjugated chlorhexidine nanoparticles and chlorhexidine alone exhibited amoebistatic effects. Briefly, *A. castellanii* (5×10^5 amoebae) organisms were incubated with various concentrations of Au-conjugated chlorhexidine nanoparticles and chlorhexidine alone for 48 h at 37°C as described in Materials and Methods. The next day, amoeba counts were determined by hemocytometer counting. Note that Au-conjugated chlorhexidine nanoparticles at 5 μM concentration, but not chlorhexidine alone at 5 μM concentration, exhibited significant inhibitory effects on *A. castellanii* growth compared to that of amoebae incubated in solvent alone ($P < 0.05$ using 2-sample t test with two-tailed distribution). The dotted bar indicates the original inoculum. The results are expressed as the means ± standard errors from three independent experiments performed in duplicate.
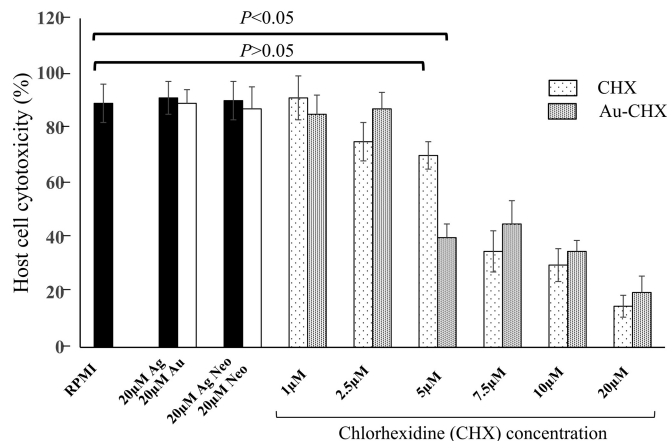
the cellular integrity, resulting in leakage and, finally, cell death. Enhanced effects of Au-conjugated chlorhexidine also may be explained by the fact that, in addition to chlorhexidine effects on parasite membranes, metals such as Ag or Au affect DNA replication ability and the expression of ribosomal subunit proteins and enzymes involved in ATP production or enzymes involved in the respiratory chain (11); however, the precise mechanism of enhanced amoebicidal effects of Au-conjugated chlorhexidine still is not well understood. It is also possible that nanoparticles of Au-conjugated chlorhexidine are taken up (via phagocytosis) and/or retained more effectively than with chlorhexidine alone. Another likely explanation is that Au conjugation allows interaction with thiols, providing an effective and selective means of controlled intracellular release to affect amoeba viability. Au nanoparticles alone or Ag-conjugated neomycin had no effects, suggesting that cytotoxic effects are due to chlorhexidine. Chlorhexidine conjugated with gold at 5 μM showed significantly higher growth-inhibitory effects than chlorhexidine alone. When PYG is the medium, it is reasonable to suggest that nanoparticles of Au-conjugated chlorhexidine are taken up and/or retained better (via phagocytosis) than chlorhexidine alone (25, 26), which may explain the increased recovery of chlorhexidine-treated amoebae after 48 h of incubation.

Pretreatment of amoebae with 5 μM Au-conjugated chlorhexidine, but not chlorhexidine alone, protected host cells against *A. castellanii*-mediated cytotoxicity. Of note, 7.5 μM Au-conjugated chlorhexidine also exhibited levels of protection similar to those seen for 5 μM. When chlorhexidine alone was used (Fig. 5), there was no difference between 5 μM and 7.5 μM ($P > 0.05$). However, when we compared data to those for the control (no drug), a significant difference was observed only with 7.5 μM and not 5 μM. When Au-conjugated chlorhexidine was studied (Fig. 5), again there was no difference between 5 μM and 7.5 μM

($P > 0.05$). However, when we compared data to those for the control (no drug), significant difference was observed at both 5 μM and 7.5 μM. This was consistent with amoebicidal findings reported in Fig. 3. Based on these data, we conclude that the conjugation of chlorhexidine with nanoparticles enhances their anti-amoebic efficacy, as we are able to see differences in protection against host cell cytotoxicity at lower concentrations of the drug.

Although *in vivo* studies are needed to further assess their efficacy, these findings confirm that nanoparticles are promising carriers in enhancing chemotherapeutic effects of the present drugs. They provide enhanced stability, tuneable surface conjugation chemistry, monodisperse size distribution, physicochemical properties, higher drug loading, controlled drug release, improved pharmacokinetics, and dual effects of drug agent and nanoparticles, which suggests that nanotechnology together with available antiamoebic compounds will offer effective and less toxic options to patients for the treatment of *Acanthamoeba* infections.

REFERENCES

1. **Khan NA.** 2006. *Acanthamoeba*: biology and increasing importance in human health. FEMS Microbiol Rev **30**:564–595. http://dx.doi.org/10.1111/j.1574-6976.2006.00023.x.
2. **Marciano-Cabral F, Cabral G.** 2003. *Acanthamoeba* spp. as agents of disease in humans. Clin Microbiol Rev **16**:273–307. http://dx.doi.org/10.1128/CMR.16.2.273-307.2003.
3. **Visvesvara GS, Moura H, Schuster FL.** 2007. Pathogenic and opportunistic free-living amoebae: *Acanthamoeba* spp., *Balamuthia mandrillaris*, *Naegleria fowleri*, and *Sappinia diploidea*. FEMS Immunol Med Microbiol **50**:1–26. http://dx.doi.org/10.1111/j.1574-695X.2007.00232.x.
4. **Ficker L, Seal D, Warhurst D, Wright P.** 1990. *Acanthamoeba* keratitis–resistance to medical therapy. Eye (Lond) **4**:835–838. http://dx.doi.org/10.1038/eye.1990.132.
5. **Perez-Santonja JJ, Kilvington S, Hughes R, Tufail A, Metheson M, Dart JKG.** 2003. Persistently culture positive *Acanthamoeba* keratitis; *in vivo* resistance and *in vitro* sensitivity. Ophthalmology **110**:1593–1600. http://dx.doi.org/10.1016/S0161-6420(03)00481-0.
6. **Ehlers N, Hjortdal J.** 2004. Are cataract and iris atrophy toxic complications of medical treatment of *Acanthamoeba* keratitis? Acta Ophthalmol Scand **82**:228–231. http://dx.doi.org/10.1111/j.1600-0420.2004.00237.x.
7. **Casper T, Basset D, Leclercq C, Fabre J, Peyron-Raison N, Reynes J.** 1999. Disseminated *Acanthamoeba* infection in a patient with AIDS: response to 5-fluorocytosine therapy. Clin Infect Dis **29**:944–945. http://dx.doi.org/10.1086/520471.
8. **Migueles S, Kumar P.** 1998. Primary cutaneous *Acanthamoeba* infection in a patient with AIDS. Clin Infect Dis **27**:1547–1548. http://dx.doi.org/10.1086/517750.
9. **Sharma R, Jhanji V, Satpathy G, Sharma N, Khokhar S, Agarwal T.** 2013. Coinfection with *Acanthamoeba* and *Pseudomonas* in contact lens-associated keratitis. Optom Vis Sci **90**:e53–e55. http://dx.doi.org/10.1097/OPX.0b013e31827f15b4.
10. **Fresta M, Puglisi G, Giammona G, Cavallaro G, Micali N, Furneri PM.** 1995. Pefloxacine mesilate- and ofloxacin-loaded polyethylcyanoacrylate nanoparticles: characterization of the colloidal drug carrier formulation. J Pharm Sci **84**:895–902. http://dx.doi.org/10.1002/jps.2600840721.
11. **Pal S, Tak YK, Song JM.** 2007. Does the antibacterial activity of silver nanoparticles depend on the shape of the nanoparticle? A study of the Gram-negative bacterium *Escherichia coli*. Appl Environ Microbiol **73**:1712–1720.
12. **Sondi I, Salopek-Sondi B.** 2004. Silver nanoparticles as antimicrobial agent: a case study on *E. coli* as a model for Gram-negative bacteria. J Colloid Interface Sci **275**:177–182. http://dx.doi.org/10.1016/j.jcis.2004.02.012.
13. **Aqeel Y, Siddiqui R, Anwar A, Shah MR, Khoja S, Khan NA.** 2015. Photochemotherapeutic strategy against *Acanthamoeba* infections. Antimicrob Agents Chemother **69**:3031–3041.
14. **Alsam S, Kim KS, Stins M, Rivas AO, Sissons J, Khan NA.** 2003. *Acanthamoeba* interactions with human brain microvascular endothelial cells. Microb Pathog **35**:235–241. http://dx.doi.org/10.1016/j.micpath.2003.07.001.
15. **Stins MF, Gilles F, Kim KS.** 1997. Selective expression of adhesion molecules on human brain microvascular endothelial cells. J Neuroimmunol **76**:81–90. http://dx.doi.org/10.1016/S0165-5728(97)00036-2.
16. **Aqeel Y, Siddiqui R, Manan Z, Khan NA.** 2015. The role of G protein coupled receptor-mediated signaling in the biological properties of *Acanthamoeba castellanii* of the T4 genotype. Microb Pathog **81**:22–27. http://dx.doi.org/10.1016/j.micpath.2015.03.006.
17. **Borazjani RN, May LL, Noble JA, Avery SV, Ahearn DG.** 2000. Flow cytometry for determination of the efficacy of contact lens disinfecting solutions against *Acanthamoeba* spp. Appl Environ Microbiol **66**:1057–1061. http://dx.doi.org/10.1128/AEM.66.3.1057-1061.2000.
18. **Lakhundi S, Khan NA, Siddiqui R.** 2014. The effect of environmental and physiological conditions on excystation of *Acanthamoeba castellanii* belonging to the T4 genotype. Parasitol Res **113**:2809–2816. http://dx.doi.org/10.1007/s00436-014-3941-6.
19. **El-Ansary A, Al-Daihan S.** 2009. On the toxicity of therapeutically used nanoparticles: an overview. J Toxicol **2009**:754810. http://dx.doi.org/10.1155/2009/754810.
20. **Connor EE, Mwamuka J, Gole A, Murphy CJ, Wyatt MD.** 2005. Gold nanoparticles are taken up by human cells but do not cause acute cytotoxicity. Small **1**:325–327. http://dx.doi.org/10.1002/smll.200400093.
21. **Ghosh P, Han G, De M, Kim CK, Rotello VM.** 2008. Gold nanoparticles in delivery applications. Adv Drug Deliv Rev **60**:1307–1315. http://dx.doi.org/10.1016/j.addr.2008.03.016.
22. **Pissuwan D, Niidome T, Cortie MB.** 2009. The forthcoming applications of gold nanoparticles in drug and gene delivery systems. J Control Release **149**:65–71.
23. **Pérez-Herrero E, Fernández-Medarde A.** 2015. Advanced targeted therapies in cancer: drug nanocarriers, the future of chemotherapy. Eur J Pharm Biopharm **93**:52–79. http://dx.doi.org/10.1016/j.ejpb.2015.03.018.
24. **Dykman LA, Khlebtsov NG.** 2011. Gold nanoparticles in biology and medicine: recent advances and prospects. Acta Nat **3**:34–55.
25. **Weisman RA, Korn ED.** 1967. Phagocytosis of latex beads by *Acanthamoeba*. I. Biochemical properties. Biochemistry **6**:485–497.
26. **Korn ED, Weisman RA.** 1967. Phagocytosis of latex beads by *Acanthamoeba*. II. Electron microscopic study of the initial events. J Cell Biol **34**:219–227.